

Optimal Configuration and Planning of Distributed Energy Systems Considering Renewable Energy Resources

H. Taraghi Nazloo¹, R. Babazadeh^{1*}, and M. Varmazyar²

¹ Faculty of Engineering, Urmia University, Urmia, West Azerbaijan 5756151818, Iran

² Department of Industrial Engineering, Sharif University of Technology, Tehran 1458889694, Iran

Received 13 December 2022; revised 02 May 2023; accepted 02 August 2023; published online 05 January 2024

ABSTRACT. With increasing electricity demand, conventional centralized power generation systems encounter numerous challenges, including transmission and distribution losses, limited capacity, and high operational costs. In response, distributed energy systems have emerged as a promising solution by enabling electricity generation in close proximity to consumption points. These systems leverage renewable energy sources and minimize energy losses during transmission, presenting a more sustainable and efficient alternative. By utilizing diverse energy sources such as solar thermal panels, photovoltaic systems, geothermal energy, distributed energy systems enhance overall efficiency, and reduce power losses during transmission as well as greenhouse gas emissions. This research endeavor presents a novel approach employing mixed-integer linear programming to optimize distributed energy systems. The proposed model facilitates the determination of optimal dimensions of technologies, including combined heat and power systems, boilers, electric chillers, and absorption chillers, while simultaneously minimizing total costs and greenhouse gas emissions and adhering to real-world constraints. The findings of this study are validated through a real-world numerical example, confirming the model's efficiency in configuring and planning distributed energy systems optimally, thereby enhancing their operational performance.

Keywords: distributed energy systems, renewable energy, optimization, microgrids

1. Introduction

In contemporary society, energy is vital in various human activities such as transportation, heat, lighting, and cooking. Electricity, as an essential secondary energy resource, can be generated from both renewable sources, such as hydropower, wind turbines, and photovoltaic panels, as well as non-renewable sources, including coal, petroleum, and natural gas (Demirhan, 2022; Giacosa and Walker, 2022). However, the utilization of fossil fuels for electricity production has significant adverse consequences on air quality, human health, and the environment, consequently exacerbating global warming, with coal power emerging as a particularly pressing concern (Anyaoha and Zhang, 2022; Mei et al., 2022).

Addressing the concern of reducing greenhouse gas (GHG) emissions and economic growth is a potent challenge. Mitigating GHG emissions often requires reducing the reliance on fossil fuels, as these fuels contribute to human-made emissions (Amanatidou et al., 2023). Nonetheless, since numerous countries are still heavily dependent on fossil fuels as their primary energy source, it presents a major worldwide issue (Papież et al., 2022). Therefore, it becomes crucial in modern society to

actively investigate and advance alternative energy sources capable of efficiently substituting fossil fuels and guaranteeing sustainable energy production.

To effectively tackle climate change and meet emission targets, it is essential for policymakers to thoroughly examine greenhouse gas emissions dynamics, evaluate their environmental impacts, and assess existing mitigation policies. Governments should prioritize reducing fossil fuel usage and curbing greenhouse gas emissions as part of their strategies (Guibentif and Vuille, 2022). Innovative structures reliant on sustainable and eco-friendly renewable energy resources like solar, wind, and microgrids (MGs) need to be developed to mitigate the adverse effects of traditional energy systems. Photovoltaic (PV) and wind turbine (WT) technology can provide reliable power sources, especially for remote areas with high transmission costs (Bukar et al., 2020; Ahmadi and Rezaei, 2021). However, integrating intermittent and unpredictable renewable power sources into energy strategies can be quite challenging. MGs offer a viable solution by establishing a local energy network incorporating renewable generation, energy storage, and distributable resources (Chen et al., 2022).

MGs offer a promising solution to provide electricity to remote areas, minimizing transmission line losses and enhancing overall power grid efficiency (Chaudhary et al., 2021). Consequently, there has been a significant focus on the research and development of MGs, aiming to balance electricity distribution,

* Corresponding author. Tel.: +98 44 32972854; fax: +98 44 32773591.
E-mail address: r.babazadeh@urmia.ac.ir (R. Babazadeh).

environmental conservation, and cost-effectiveness. These systems utilize renewable energy sources and energy storage components to maintain stable voltage levels in grid-connected or islanded modes (Wei et al., 2020). In the grid-connected mode, the primary grid governs the voltage and frequency of the microgrid (MG), while converters regulate voltage in the islanded mode. Frequency management follows a hierarchical design similar to a power system (Rios and Garces, 2022).

MGs offer a multitude of benefits across technical, economic, environmental, and social aspects (Taraghi Nazloo et al., 2023). These advantages include mitigating environmental impacts by utilizing renewable energy technologies, enhancing efficiency through combined heat and electricity systems, improving energy management and voltage control, promoting social welfare, and bolstering system reliability and flexibility (Ahmethodzic and Music, 2021). However, MGs face certain challenges, notably the high upfront costs of installing renewable energy systems and energy storage equipment. Additionally, ensuring the cybersecurity of MGs is another critical concern due to their dependence on advanced digital systems and control mechanisms, which are vulnerable to cyberattacks (Hu et al., 2022).

Various techniques including simulation, management approaches, and mathematical modeling can be employed to tackle MG planning issues. Among these, mathematical modeling shows superior capability due to its ability to accurately represent real-world situations, facilitate faster and more precise decision-making, provide precise solutions, and offer enhanced flexibility. As a result, this study proposes mathematical modeling as a workable option for medium-term planning of grid-connected MGs.

The main contribution of this research includes introducing a novel mixed integer linear programming (MILP) model for optimization of the configuration and planning of distributed energy systems (DESS). The model considers different energy sources like solar thermal panels (ST), PV systems, and geothermal technologies, as well as the optimal size of technologies, such as combined heat and power (CHP) systems, boilers, electric chillers (EC), and absorption chillers (AC). Based on the literature review table (Table 1) and to the best of our knowledge, there is no available research in the literature on application of all mentioned resources in this article together. Also, decisions such as electricity transmission, selling and purchasing from the grid, heat and cold generation, and required natural gas for certain technologies are optimized through the proposed model. The model's main objective is to reduce overall costs and GHG emissions while meeting power demand and production limits for renewable energy. The proposed model is verified and validated through a real case study inspired by the literature.

The body of the paper is divided into the following sections: In Section 2, a systematic literature review is performed. In Section 3, the model is described and mathematically formulated. The results of the simulations and discussions are reported in Section 4. The main findings, as well as future suggestions, are presented in Section 5.

2. Literature Review

Studying the integration of distributed energy resources in operational distribution approaches has amplified the potential of utilizing methods like MGs to mitigate electricity supply disruptions and enhance grid stability against faults and other challenges (Adewole et al., 2022). Extensive research has been conducted on MG planning to improve performance and flexibility, reduce costs and pollutant emissions, and maximize the adoption of renewable energy sources through diverse mathematical programming and modeling approaches (Guo et al., 2020). For instance, there is a notable example of research on MGs dating back to the 1700s, specifically focusing on the comprehensive design of MG energy storage with guaranteed optimality.

As depicted in Figure 1, research on MGs has witnessed a notable surge in attention over the past 21 years, establishing itself as a significant study area. Tahiri et al. (2021) conducted a study focusing on the optimal management and control strategies for an isolated hybrid solar-wind-battery-diesel power system. Their approach utilized simulations to optimize the energy management and control of the system, ensuring efficient and cost-effective operation. Similarly, Mathiesen et al. (2021) presented a novel method for achieving dispatch planning to address intra-hour variability. They introduced a power balance approach for optimizing MG demand within shorter time intervals. The results provide evidence of the enhanced optimization of MGs by utilizing the power balance method. MGs are increasingly recognized as cost-effective clusters incorporating many direct currents. Present circumstances highlight that cyberattacks pose a significant threat to the reliability and flexibility of the power system. To address this, Pinto et al. (2021) introduced a robust model for development planning involving multiple MGs, distributed power sources, market response, and generation options. The model, solved through a two-stage robust optimization technique, offers practical growth planning recommendations and optimal daily operations. In a similar vein, Dumas et al. (2021) proposed a robust function-based application strategy for sharing data between operational planning and real-time optimization. This approach offers benefits such as reducing predictable errors, minimizing total costs, and improving MG revenue. However, achieving the optimal configuration of off-grid MGs in developing countries is challenging due to various approaches and socio-economic risks that may discourage private sector investment. To address these challenges, Fioriti et al. (2021) proposed a specific stochastic dynamic strategy for sizing MGs, effectively considering system performance and accounting for the inherent uncertainty in load development. Similarly, Phommixay et al. (2021) presented a two-stage approach to minimize the overall expenses of MGs considering uncertainty in energy demand and planned outages. Aluisio et al. (2021) developed a methodology for assessing MG structures' sizing, performance, and reliability, incorporating PV and energy storage technologies. They employed a MILP approach for techno-economic planning of MGs, aiming to optimize operational scenarios. Basu (2021) introduced a mathematical model incorporating heat demand

Table 1. Comparison of the Existing Works in the Literature

Authors	Object function		Model conditions		Model type	Approach	Used resources	Software
	Single	Multi	Uncertain	Certain				
Wei et al. (2020)	✓		✓		Maximization	Used gap decision and the two-line analysis algorithm	PV, WT, batteries, electric heaters, and CHP	MATLAB
Bukar et al. (2020)	✓		✓		Minimization	Used GOA algorithm	WT, PV, battery, load converter, and diesel generator	MATLAB
Kiptoo et al., (2020)	✓		✓		Minimization	Used isolated MGs	WT, PV, battery, heat pump storage system, and diesel generator	MATLAB
Oviedo-Cepeda et al. (2020)	✓		✓		Minimization	Used convex programming	Diesel generators, batteries, and PV	MATLAB
Jiao et al. (2020)		✓	✓		Maximization	Used semi-entropy model	Battery, PV, WT, and diesel generator	MATLAB
Roy et al. (2021)	✓			✓	Maximization	Suggested a two-level optimization	Fuel cell, PV, and battery	MATLAB
Águila et al. (2021)	✓		✓		Minimization	Multi-criteria decision algorithm	WT, PV, battery, load converter, and diesel generator	MATLAB
Doucier et al. (2021)	✓		✓		Minimization	Genetic algorithm	WT, PV, and battery	MATLAB
Shezan et al. (2022)	✓			✓	Minimization	Used freestanding hybrid MG	Solar diesel generator, PV, battery storage, and WT	HOMER
Gabriel et al. (2022)		✓	✓		Minimization	Used genetic algorithm and particle swarm	Diesel engine generators, battery, PV, and WT	MATLAB
Bukar et al. (2022)	✓		✓		Minimization	Law-based algorithm and search technique	WT, PV, battery, load converter, and diesel generator	MATLAB
Bayati et al. (2022)	✓		✓		Minimization	Used DC MG and support vector machines	Fuel cells, batteries, PV, and WT	PYTHON
Villa and Henao (2022)	✓		✓		Maximization		PV	LINGO
This paper	✓			✓	Minimization	MILP to model DES, considering various types of renewable energy resources	PV, grid power, geothermal, CHP, boiler, ST, EC, and AC	GAMS

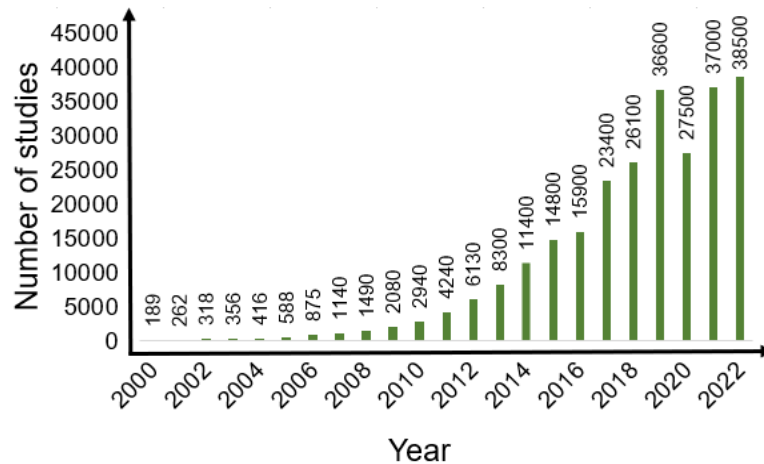


Figure 1. Comparison of the number of studies in the last 23 years.

and increasing energy and heat production rates in isolated MGs. The model seeks cost-effective and reliable development strategies to meet electricity and heat demand.

In today's world, reducing GHG emissions is a significant global challenge. Harrold et al. (2022) employ carbon-free renewable energy sources (PV and WT), multi-agent reinforcement learning, and a multi-agent deep deterministic policy gradient algorithm for effective GHG management. Electric vehicles (EVs) are a rapidly advancing technology that can contribute to reducing emissions in transportation and power sectors. Balasubramanian et al. (2022) provide an overview of hydrogen as an alternative fuel, highlighting its thermodynamic behavior and discussing its benefits, properties, and production methods. O'Neill et al. (2022) focus on the annual operation and demonstrate the advantages of EVs and Vehicle-to-Grid in MG environments and processes. Califano et al. (2022) present a novel concept of an integrated MG incorporating renewable energy sources, power storage, and a reversible solid oxide cell system. Their approach ensures that the energy produced within the MG is efficiently utilized. To address the challenge of long-term energy outages in the central grid, Kizito et al. (2022) propose an MG mathematical model, incorporating financial, technical, and investment factors, and suggest a multi-stage stochastic plan. Bartels et al. (2022) investigate the impact of hydrogen on the electric grid and MG investment costs, revealing that introducing hydrogen in the MG reduces investment expenses and enhances efficiency. A comprehensive review of studies conducted in this field, summarized in Table 1, will be discussed further.

The literature review conducted in this study reveals notable gaps in the current understanding of DESs, including:

- Insufficient comprehensive approaches for optimizing the configuration and planning of DESs, considering renewable energy sources, heat, cool, and electricity generation.
- The necessity to reduce reliance on fossil fuels and mitigate air pollution through the promotion of distributed energy generation technology as a viable solution to upcoming challenges like fossil fuel depletion and environmental concerns.

3. Problem Description and Mathematical Formulation

This study aims to optimize a DES by employing a MILP approach. The proposed model considers various renewable energy sources and aims to minimize total investment costs, planning costs, and GHG emissions. The model makes decisions regarding installing different equipment types, including CHPs, PVs, boilers, ST panels, ECs, and ACs. Figure 2 depicts the potential connections between nodes supplying electricity, heat, and cool energy within the DES. CHP technology is utilized for both electricity and heat generation, while a boiler is employed for heat production. Geothermal energy contributes to electricity and heat generation, while PVs and upstream grids are used for electricity generation. Heat generated by CHPs and boilers is distributed to areas with heat demand, and

ACs and chillers provide cooling. ST equipment serves the purpose of heat and cold production. The MILP approach facilitates determining the optimal combination and utilization of available technologies within the central energy system.

3.1. Assumptions

The proposed MILP model is developed based on a set of underlying assumptions, which include the following:

- The possibility of energy demand shortages, necessitating the calibration of associated penalties based on decision-makers' preferences.
- The fixed and known location of the geothermal node, determined by the characteristics of the case study.
- The deterministic and known parameters of the proposed model.
- Allowing for electricity transmission between different nodes to minimize transmission losses.
- Allowing for the buying and selling of electricity to and from the utility grid.
- While the capacities of various technologies are predetermined, the proposed model makes decisions regarding the installation of technologies across different nodes.

3.2. Mathematical Model

The objective of the proposed mathematical model is to minimize the overall cost of the MG while taking into account constraints that accurately represent real-world challenges and considerations. Nomenclature used to develop the proposed model has been presented in Appendix A.

3.2.1. Objective Function

The main aim of this model is to minimize the total cost of the MG by considering five criteria: investment costs (C_{inv}), operation and maintenance costs (C_{op}), electricity transmission costs (C_{TR}), carbon emission costs (C_{mis}) and penalties for failing to meet electricity, heat, and cool demand. These criteria are integrated to determine the optimal solution for all buildings in the area:

$$C_{total} = C_{inv} + C_{op} + C_{TR} + C_{mis} + \sum_y \sum_t \sum_h \sum_n (PEN^C \times UM_{y,t,h,n}^C + PEN^H \times UM_{y,t,h,n}^H + PEN^E \times UM_{y,t,h,n}^E) \quad (1)$$

In the proposed model, the objective function aims to minimize the total cost of the MG. This cost includes the initial costs associated with system implementation, such as installing desired technologies and wiring. The total investment cost is the first term in Equation (1), which captures the overall cost of implementing the MG system. Equation (2) further breaks down the investment cost by considering the individual costs of PV, CHP, ST, boiler, AC, and EC technologies. Each tech-

nology cost is multiplied by a binary variable that indicates whether the technology is installed in the respective nodes. The wiring cost is also considered, which is calculated based on the distance between nodes and the expenditure associated with wire installation. Lastly, a binary variable, $U_{n,n'}$, is included in the last term of Equation (2) to indicate whether a wire is installed between nodes n and n' , allowing for electricity exchange between nodes in the residential area:

$$C_{inv} = \sum_n C^{PV} \times MS_n^{PV} + \sum_l \sum_n C_l^{CHP} \times X_{l,n}^{CHP} + \sum_n C^{ST} \times MS_n^{ST} + \sum_b \sum_n C_b^B \times Y_{b,n}^B + \sum_n C^{AC} \times g_n^{AC} + \sum_n C^{EC} \times g_n^{EC} + \sum_n \sum_{n'} (C_{n,n'} \times DI_{n,n'} \times U_{n,n'}) \quad (2)$$

In Equation (3), the model calculates the operation and maintenance costs of the various technologies. This includes determining the cost of operating PV for electricity production, which is obtained by multiplying the electricity production from PV by its respective operation cost. Similar calculations are performed for CHP types, ST for heat production, and boilers. The operational cost of cold production from ST and both types of chillers, as well as the operating cost of heat production in CHP types, are also calculated similarly. By considering these costs, the total operational and maintenance cost of the MG can be determined:

$$C_{op} = \sum_y \sum_t \sum_h \sum_n C1_{y,t,h,n}^{PV} \times OP_{y,t,h,n}^{PV} + \sum_y \sum_t \sum_h \sum_l \sum_n C1_{y,t,h,l,n}^{CHP} \times OP_{y,t,h,l,n}^{CHP} + \sum_y \sum_t \sum_h \sum_n C1_{y,t,h,n}^{ST} \times OH_{y,t,h,n}^{ST} + \sum_y \sum_t \sum_h \sum_n C1_{y,t,h,n}^{ST} \times OC_{y,t,h,n}^{ST} + \sum_y \sum_t \sum_h \sum_b \sum_n C1_{y,t,h,b,n}^B \times OH_{y,t,h,b,n}^B + \sum_y \sum_t \sum_h \sum_n C1_{y,t,h,n}^{AC} \times OC_{y,t,h,n}^{AC} + \sum_y \sum_t \sum_h \sum_n C1_{y,t,h,n}^{EC} \times OC_{y,t,h,n}^{EC} + \sum_y \sum_t \sum_h \sum_l \sum_n C1_{y,t,h,l,n}^{CHP} \times OH_{y,t,h,l,n}^{CHP} \quad (3)$$

Equation (4) accounts for the cost of power transmission between nodes (C_{TR}). It encompasses the cost associated with electricity transmission between nodes n and n' by CHP and PV technologies:

$$C_{TR} = \sum_y \sum_t \sum_h \sum_l \sum_n \sum_{n'} C_{y,t,h,l,n,n'}^{TRCHP} \times TR_{y,t,h,l,n,n'}^{CHP} + \sum_y \sum_t \sum_h \sum_n \sum_{n'} C_{y,t,h,n,n'}^{TRPV} \times TR_{y,t,h,n,n'}^{PV} \quad (4)$$

The model's objective is cost minimization, not optimizing carbon emissions. Equation (5) accounts for the cost associated with carbon emission penalties resulting from installing boiler and CHP technologies in all nodes. By including this term in the objective function, the model encourages selecting technologies with lower carbon emissions, as higher emissions would lead to increased penalty costs:

$$C_{mis} = \sum_y \sum_t \sum_h \sum_b \sum_n PEN^{CA} \times OH_{y,t,h,b,n}^B \times \alpha + \sum_y \sum_t \sum_h \sum_l \sum_n PEN^{CA} \times OP_{y,t,h,l,n}^{CHP} \times \delta + \sum_y \sum_t \sum_h \sum_l \sum_n PEN^{CA} \times OH_{y,t,h,l,n}^{CHP} \times \mu \quad (5)$$

3.2.2. Constraints

Energy balance constraints ensure that the total energy generated by the MG is equal to the total energy consumed by the buildings, ensuring efficient energy management and cost optimization. Buying and selling of electricity constraints enable the MG to engage in transactions with the grid, allowing it to purchase electricity when the demand exceeds the MG's generation capacity and sell excess electricity when there is surplus production. Capacity constraints restrict the maximum capacity of each technology that can be installed in the MG, preventing overloading and ensuring optimal utilization of resources. Shortage constraints are implemented to guarantee that the energy demands of the buildings are met even in situations where the MG's production falls short. These constraints ensure an uninterrupted energy supply to the buildings by allowing the MG to import additional electricity from the grid to cover any energy deficits.

(1) Energy balances: Equation (6) in the proposed model guarantees a balanced and efficient energy system by ensuring that the total electricity generated by the installed technologies, such as PV, CHP types, and geothermal, is sufficient to meet the MG's electricity demand. It also accounts for any shortages that may occur and considers electricity transmission between nodes and grid interactions. This constraint plays a crucial role in maintaining the stability and equilibrium of the MG, while simultaneously optimizing cost and reducing carbon emissions:

$$OP_{y,t,h,n}^{PV} + \sum_l OP_{y,t,h,l,n}^{CHP} + OP_{y,t,h,n}^G + PE_{y,t,h,n} - \sum_l AE_{y,t,h,l,n}^{CHP} - AE_{y,t,h,n}^{PV} - \sum_{l,n'} TR_{y,t,h,l,n,n'}^{CHP} - \sum_{n'} TR_{y,t,h,n,n'}^{PV} + \sum_{l,n'} TR_{y,t,h,l,n',n}^{CHR} + \sum_{n'} TR_{y,t,h,n',n}^{PV} \geq Dem_{y,t,h,n}^E - UM_{y,t,h,n}^E, \forall y,t,h,n \quad (6)$$

Equation (7) in the model ensures a balanced heat flow within the MG by requiring that the total heat generated by the installed technologies (boiler, CHP, ST, and geothermal) and any heat shortage is sufficient to meet the heat demand of the buildings, including the additional heat required for the AC tech-

nology. This constraint guarantees that the MG can effectively fulfill the heat requirements while considering the specific needs of the AC technology:

$$\sum_b OH_{y,t,h,b,n}^B + OH_{y,t,h,n}^{ST} + \sum_l \frac{OH_{y,t,h,l,n}^{CHP}}{HR_l} + UM_{y,t,h,n}^H + OH_{y,t,h,n}^G \geq DH_{y,t,h,n} + \frac{DH_{y,t,h,n}^{AC}}{COP^{AC}}, \forall y,t,h,n \quad (7)$$

Equation (8) maintains the balance of cool flows within the nodes by stipulating that the combined cold production from AC, EC, and ST technologies, along with any cool deficiency, should be equal to or greater than the cool demand. This constraint guarantees that the total cool supply is sufficient to meet the cool demand, accounting for any shortage that may need to be fulfilled by purchasing cool energy from the grid:

$$OC_{y,t,h,n}^{AC} + OC_{y,t,h,n}^{EC} + OC_{y,t,h,n}^{ST} + UM_{y,t,h,n}^C \geq DC_{y,t,h,n}, \forall y,t,h,n \quad (8)$$

(2) Equipment's capacity: Equation (9) calculates the electrical energy generation of each CHP technology by considering its capacity, electrical efficiency coefficient, and the specific node, time period, and year:

$$OP_{y,t,h,l,n}^{CHP} \leq WA_l^{CHPE} \times \theta_l^{CHPE} \times X_{l,n}^{CHP}, \forall y,t,h,l,n \quad (9)$$

Equation (10) enforces installing a single CHP technology per node, prohibiting the simultaneous installation of multiple CHP technologies within the same node. This constraint ensures that each node is equipped with only one CHP unit:

$$\sum_l X_{l,n}^{CHP} \leq 1 \quad (10)$$

Equation (11) limits the electricity output of the PV system in each node to a range determined by the performance characteristics of PV cells and the available radiation. This constraint ensures that the electricity generated by the PV system is within the feasible range based on the specific radiation conditions:

$$OP_{y,t,h,n}^{PV} \leq MS_n^{PV} \times RA_n, \forall y,t,h,n \quad (11)$$

Equation (12) restricts the surface area allocated for PV cell installation within predetermined limits. It ensures that the installed surface area of PV cells remains within the feasible range, avoiding excessive or insufficient allocation. This constraint optimizes the PV installation process while considering practicality and feasibility constraints:

$$W_n^{PV} \times LB_n^{PV} \leq MS_n^{PV} \leq UB_n^{PV} \times W_n^{PV}, \forall n \quad (12)$$

Equation (13) determines the electrical energy output of the geothermal technology, which is calculated by multiplying

the installed electrical capacity of the geothermal technology by its corresponding binary variable:

$$OP_{y,t,h,n}^G \leq WA_n^G \times \gamma_n^G, \forall y,t,h,n \quad (13)$$

Equation (14) establishes a lower limit on the production rate of the boiler, ensuring that it does not exceed its installed capacity. This constraint guarantees that the boiler operates within its capacity limitations:

$$OH_{y,t,h,b,n}^B \leq WA_{b,n}^B \times Y_{b,n}^B, \forall y,t,h,b,n \quad (14)$$

Equation (15) restricts the number of boiler units that can be installed in each node of the MG to a maximum of one. This limitation prevents unnecessary duplication of boiler capacity within a node, optimizing the system's cost-effectiveness:

$$\sum_b Y_{b,n}^B \leq 1, \forall n \quad (15)$$

Equation (16) enforces a restriction on solar thermal (ST) energy production, ensuring that it remains within the permissible range determined by the ST collector's performance and the received solar radiation. This constraint effectively manages the ST energy output, preventing excessive production and promoting optimal utilization of available solar resources:

$$OH_{y,t,h,n}^{ST} \leq MS_n^{ST} \times RA_n, \forall y,t,h,n \quad (16)$$

Equation (17) ensures that the installed capacity for solar thermal (ST) technology remains within the acceptable range, neither surpassing the maximum allowable level nor falling below the minimum allowable level:

$$LB_n^{ST} \times \lambda_n^{ST} \leq MS_n^{ST} \leq UB_n^{ST} \times \lambda_n^{ST}, \forall n \quad (17)$$

Equation (18) calculates the amount of heat energy generated by each type of CHP technology, considering their thermal efficiency coefficient and capacity for each node, period, and year:

$$OH_{y,t,h,l,n}^{CHP} \leq WA_l^{CHP} \times \beta_l^{CHP} \times X_{l,n}^{CHP}, \forall y,t,h,l,n \quad (18)$$

Equation (19) guarantees that the heat production from the geothermal technology matches its designated heat capacity:

$$OH_{y,t,h,n}^G \leq WA_n^G \times \gamma_n^G, \forall y,t,h,n \quad (19)$$

Equation (20) limits the cool production of the AC technology to be within its maximum capacity:

$$OC_{y,t,h,n}^{AC} \leq WA_n^{AC} \times g_n^{AC}, \forall y,t,h,n \quad (20)$$

Equation (21) enforces that the cool production of an EC

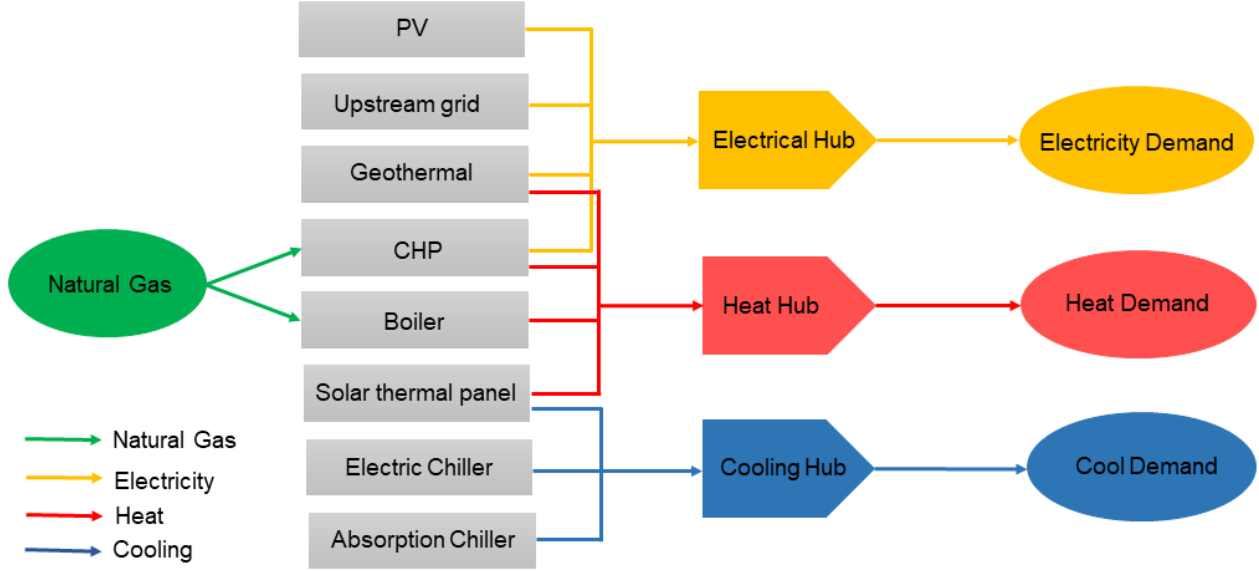


Figure 2. The structure of a distributed energy system.

technology must be equal to its maximum capacity:

$$OC_{y,t,h,n}^{EC} \leq WA_n^{EC} \times g_n^{EC}, \quad \forall y,t,h,n \quad (21)$$

Equation (22) ensures that the solar heat generated by the installed solar thermal capacity is equal to the solar radiation received:

$$OC_{y,t,h,n}^{ST} \leq MS_n^{ST} \times RA_h, \quad \forall y,t,h,n \quad (22)$$

(3) Network limitations: Equations (23) to (25) establish unidirectional power transmission by PV and CHP between nodes in the energy design model, allowing electricity flow either from node n to node n' or from node n' to node n , creating a directional graph for the network:

$$\sum_l TR_{y,t,h,l,n,n'}^{CHP} + TR_{y,t,h,n,n'}^{PV} \leq BM \times U_{n,n'}, \quad \forall y,t,h,n,n' \quad (23)$$

$$\sum_l TR_{y,t,h,l,n',n}^{CHP} + TR_{y,t,h,n',n}^{PV} \leq BM \times U_{n',n}, \quad \forall y,t,h,n',n \quad (24)$$

$$U_{n,n'} + U_{n',n} \leq 1, \quad \forall n,n' \quad (25)$$

Equation (26) guarantees the installation of either CHP or PV technology in each node, ensuring that each node has at least one of these energy generation options available:

$$U_{n,n'} \leq \sum_l X_{l,n}^{CHP} + W_n^{PV} \quad (26)$$

Equations (27) and (28) limit the power transmission through CHP and PV technologies, respectively, to be less than or equal to their respective power outputs:

$$\sum_{n'} TR_{y,t,h,l,n,n'}^{CHP} \leq OP_{y,t,h,l,n}^{CHP}, \quad \forall y,t,h,l,n \quad (27)$$

$$\sum_{n'} TR_{y,t,h,n,n'}^{PV} \leq OP_{y,t,h,n}^{PV}, \quad \forall y,t,h,n \quad (28)$$

(4) Limitations on the sale and purchase of electricity: Equations (29) and (30) restrict the electricity sold by PV and CHP technologies to be less than or equal to the electricity they produce. These constraints maintain energy balance and ensure that the model adheres to the physical feasibility:

$$AE_{y,t,h,n}^{PV} \leq OP_{y,t,h,n}^{PV}, \quad \forall y,t,h,n \quad (29)$$

$$AE_{y,t,h,l,n}^{CHP} \leq OP_{y,t,h,l,n}^{CHP}, \quad \forall y,t,h,n \quad (30)$$

Equation (31) ensures that the purchased electricity from the grid does not exceed the network's demand:

$$PE_{y,t,h,n} \leq UP_{y,t,h,n}^{PE} \times DEM_{y,t,h,n}^E, \quad \forall y,t,h,n \quad (31)$$

(5) Limitation of demand deficiency: Equations (32) to (34) are implemented to guarantee that the energy design model fulfills the electricity, heat, and cool demands without any shortage. These constraints ensure that the system's generated electricity, heat, and cool are equal to or greater than the respective required demands, eliminating any shortfall:

$$UM_{y,t,h,n}^E \leq UP_{y,t,h,n}^{DEM} \times Dem_{y,t,h,n}^E, \quad \forall y,t,h,n \quad (32)$$

$$UH_{y,t,h,n} \leq UP_{y,t,h,n}^{DEH} \times DH_{y,t,h,n}, \quad \forall y,t,h,n \quad (33)$$

$$UC_{y,t,h,n} \leq UP_{y,t,h,n}^{DEC} \times DC_{y,t,h,n}, \quad \forall y,t,h,n \quad (34)$$

4. Computational Results

The present study focuses on designing and planning DES in Meshginshar city in the Ardabil province of Iran, which significantly utilizes diverse renewable energy sources such as geothermal energy and natural gas. To enhance the efficient utilization of these renewable sources for electricity, heat, and cool generation, the study endeavors to optimize the design of a multi-energy MG in the aforementioned region. Meanwhile, some parameters of the study, such as parameters related to electric and absorption chillers, have been collected from the related works in the literature (Guo et al., 2020; Jiao et al., 2020).

The primary objective of this optimization is to reduce the dependency on conventional fossil fuels and enhance the energy system’s overall efficacy and cost-effectiveness. The findings of this study have the potential to provide critical insights and support to the decision-making bodies concerning the effective configuration and planning of the DES in the region.

4.1. Data Gathering

In this section, we introduce the input data utilized in the model, encompassing investment costs, operating costs, electricity transmission costs, equipment capacities, and demand. For example, Figure 3 provides input data for electricity demand parameters in the proposed model; showing that the electrical demand in the first year during spring and summer is higher than in the year’s second half. The peak electricity demand in spring and summer occurs from 1 to 6 pm, reaching 203,000 kWh (kilowatt hour). In autumn and winter, peak hours of electricity consumption are from 6 to 10 pm, equivalent to 117,000 kWh in the first year.

Figures S1 ~ S3 (see supporting information (SI) file) provide the proposed model’s input data for electricity, heat, and cool demand parameters. Electricity demand in the second year is higher than in the first year. In the first half of the year, peak consumption hours are from 1 to 6 pm, amounting to 269,000 kWh, while in the second half of the year, peak electricity consumption occurs from 6 to 10 hours, which is equivalent to 100,000 kWh in the second year. Figures S2 indicate that the winter season has the highest demand for heat. On average, in the first year, the heat demand during autumn is 2,264 kWh, while in winter, it is 4,588 kWh. Based on the information provided in Figures S3, it is evident that the maximum demand for cool is observed during the summer season in both the first and second years. Furthermore, the overall demand for cool during the spring and summer seasons is higher than in the autumn and winter seasons. The decision variables include the amount of electricity purchased by equipment, the electricity shortage, the amount of electricity transferred between nodes, the amount of electricity sold and generated by various sources, such as CHP, geothermal, and PV, the amount of heat produced by CHP, geothermal, boilers, and ST, as well as the amount of cold produced by AC, ST, and EC, are determined by the proposed model. Moreover, the model determined the maximum area required to install PV and ST. The obtained results are pre-

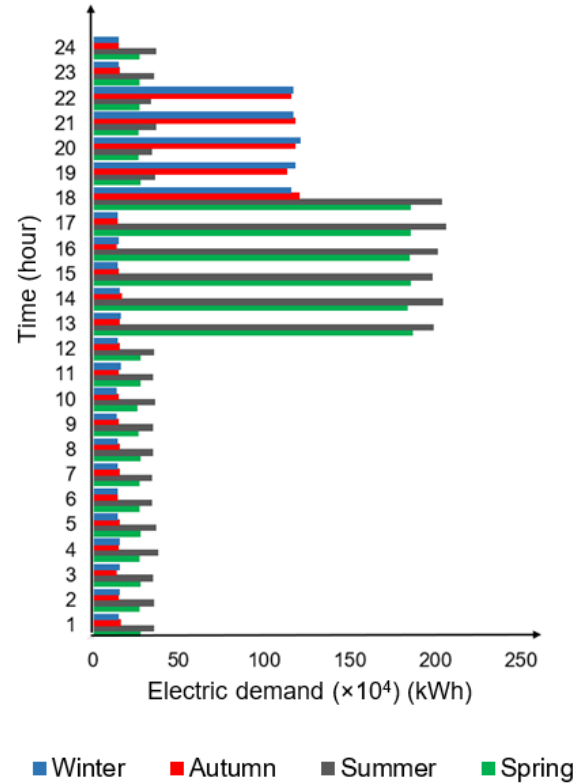


Figure 3. Electricity demand and peaks in the first year.

sented in Table S1. The tabulated data in Table S1 presents a comprehensive overview of the various types of installed technologies, namely PV, AC, EC, etc., across each node.

Table 2 presents the attributes of the distributed energy resources, comprising investment costs, electricity transmission costs, and coefficient of performance. According to Table 2, the investment cost for AC technology is 150 \$/kW, and its coefficient of performance is 0.7.

Table 3 presents the attributes and costs associated with different CHP technologies, including investment cost, transmission cost, electrical capacity, heat capacity, heat-to-power ratio, electrical efficiency coefficient, and heat efficiency coefficient. For example, the gamma type CHP exhibits an investment cost of 300 (\$/kWh), a transmission cost of 50 (\$), an electrical capacity of 720,000 (kWh), a heat capacity of 667 (kWh), a heat-to-power ratio of 6.7, an electrical efficiency coefficient of 0.6%, and a heat efficiency coefficient of 0.7%.

Table S2 provides the characteristics of the distributed energy resources, including the investment cost, electricity transmission cost, and coefficient of performance. The proposed model considers three types of boiler technology: combilers, heat-only boilers, and system boilers, each with a different investment cost of 2,600, 6,700, and 3,800 (\$/kWh), respectively. Table S2 presents detailed information about these boiler types. In the proposed model, a penalty has been incorporated for failing to meet the heat, cool, and electrical demand and for exceeding carbon emissions, as presented in Table S3.

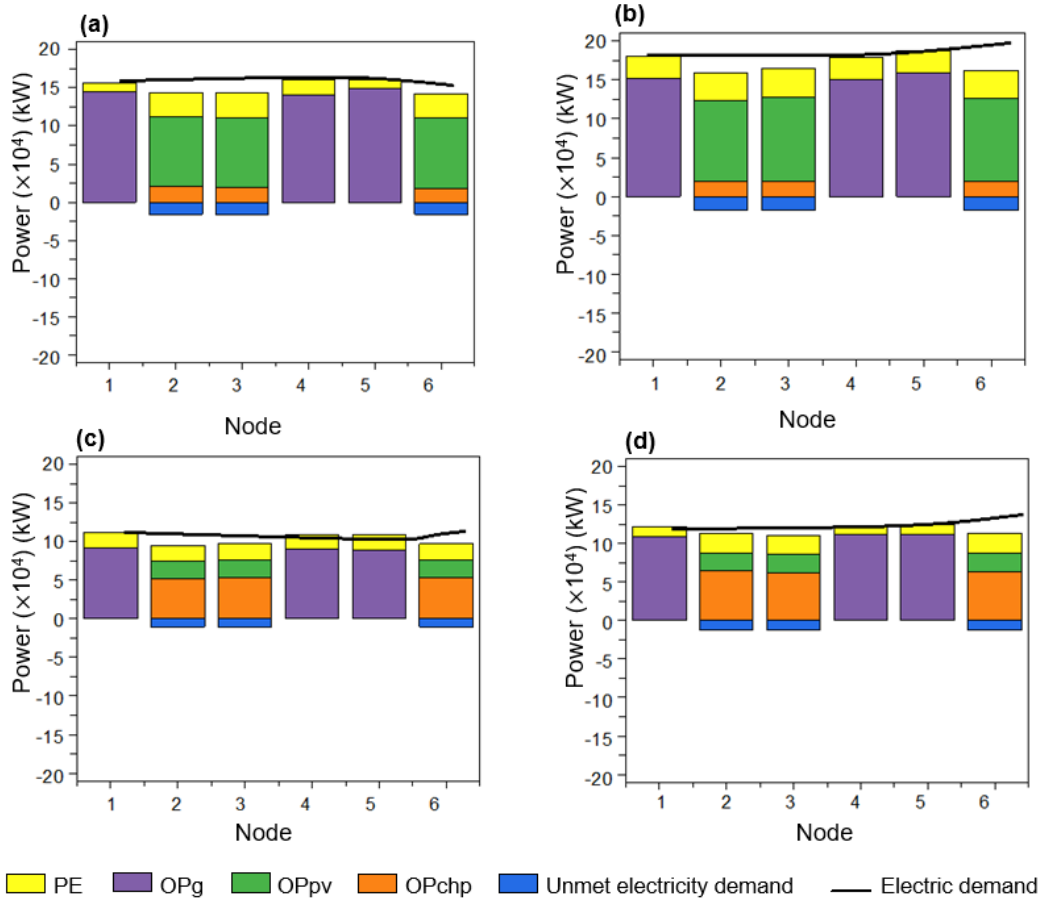


Figure 4. The amount of electricity production, demand, and shortages in the first year: (a) spring season, (b) summer season, (c) autumn season, and (d) winter season.

Table 2. Distributed Energy Resource Characteristics

Technologies	Cost item	Value	Technologies	Cost item	Value
PV	Capital investment cost for PV (C^{PV})	25 (\$/kW)	AC	Capital investment cost for AC (C^{AC})	150 (\$/kW)
	Cost of PV power transmission (C^{TRPV})	50 (\$)		Coefficient of Performance (COP)	0.7
ST	Capital investment cost for ST (C^{ST})	500 (\$/kW)			
EC	Capital investment cost for EC (C^{EC})	100 (\$/kW)			

Table 3. Specification and Costs of Different CHP Technologies

CHP technologies	Capital investment cost (\$/kW)	Cost of CHP transmission (\$)	Electrical capacity (kWh)	Heat capacity (kWh)	Heat to power ratio (HR)	θ_l^{CHPE} (%)	β_l^{CHP} (%)
Stirling engine (gamma)	300	50	720,000	667	6.7	0.60	0.70
Gas turbine	600	50	1,200,000	750	2.6	0.70	0.80
Gas turbine	800	50	960,000	667	2.3	0.80	0.85
Stirling engine (beta)	500	50	1,040,000	833	3.0	0.85	0.75

4.2. Results

The proposed model calculates the decision variables related to electricity procurement, shortages, inter-node transfers, electricity sales, and generation from different sources like CHP, geothermal, and PV. It also determines the heat production from CHP, geothermal, boilers, and ST, as well as the cold production from AC, ST, and EC. Additionally, the results are

summarized and visualized in Figures 4 to 9.

Figure 4 illustrates the first year’s electricity production, demand, and shortages. As depicted in Figures 4(a) and 4(b), the electrical demand peaks during the spring and summer months while a substantial electricity shortage occurs during the same period. Figures 4(a) and 4(b) show that nodes 2, 3, and 6 experience the most substantial deficit, with nodes 2 and

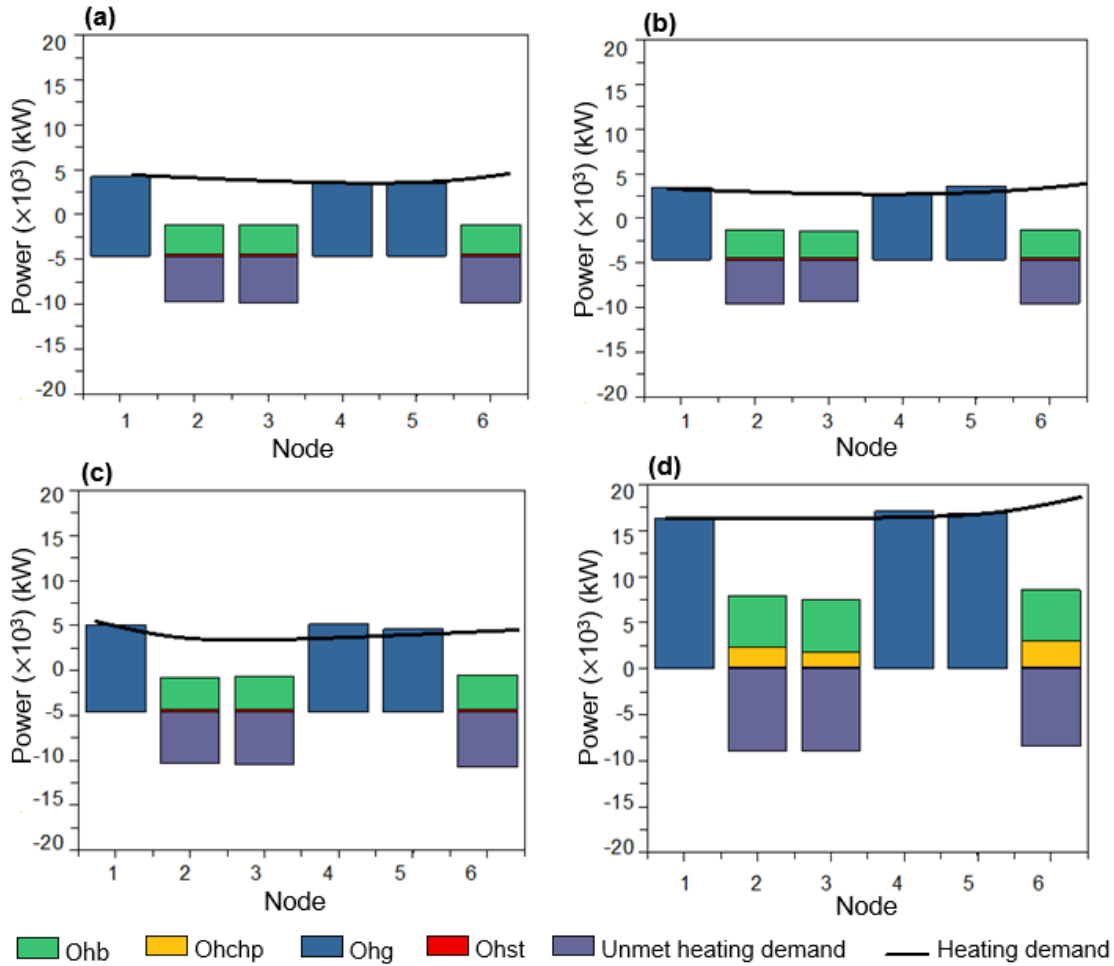


Figure 5. The amount of heat production, demand, and shortage in the first year: (a) spring season, (b) summer season, (c) autumn season, and (d) winter season.

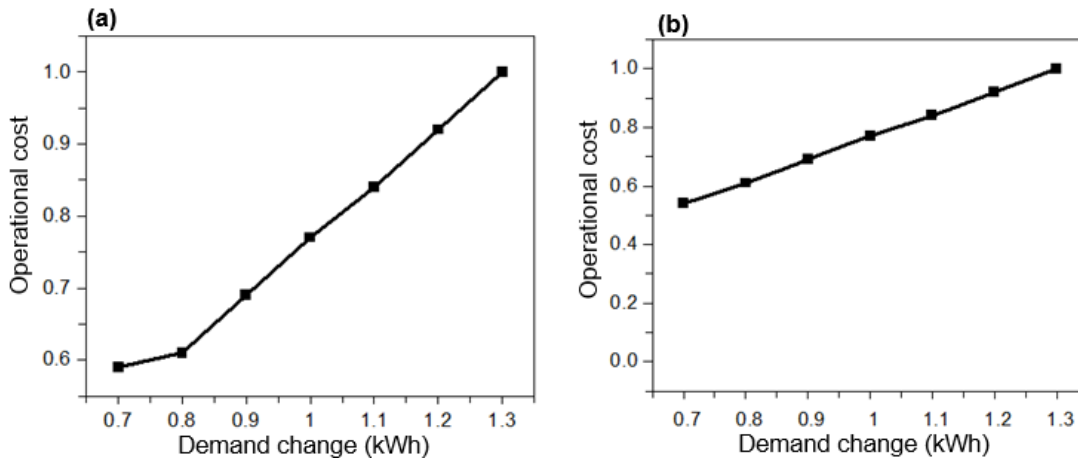


Figure 6. Demand change versus objective function and operation cost: (a) demand change versus objective function and (b) demand change versus operational cost (the horizontal axes show the percentage of nominal demand changes).

3 experiencing a deficit of 137,100 kilowatt (kW) during the spring and summer seasons and node 6 experiencing a deficit of 139,200 kW during the summer season. In contrast, it can be

observed that node 5 exhibits the highest electricity production levels through the utilization of geothermal technology, generating a total of 163,000 kW. Based on the obtained results,

a substantial proportion of the procured electricity was found to be associated with nodes 2, 3, and 6, wherein the purchased amount of electricity was recorded at 34,800 kW.

Furthermore, as shown in Figure 4, CHP technology generates lower amount of electricity in the first half of the year compared to the second half; while PV equipment generates more electricity during the same period.

Figures 4(c) and 4(d) demonstrate a discernible decline in the demand for electricity in the latter half of the year. However, it is worth noting that despite this decrease, electricity deficits continue to pose a persistent challenge across all seasons owing to their ubiquitous consumption in various industries and daily life. Notably, the summer season presents a particularly daunting challenge, as electricity shortages reach their pinnacle during this period.

Figure S4 in SI file shows an increase in electricity demand during the second year in comparison to the first year. Due to Figure S4, shows that geothermal and PV technologies are the top contributors to electricity generation during the spring and summer seasons, while CHP technology generated more electricity in the latter half of the year. Similar to the first year, Figure S4 reveals that nodes 2, 3, and 6 had the most significant amount of purchased electricity in the second year, with a total of 46,800 kW. Figures S4(a) and S4(b) illustrate that the deficiency is more pronounced in spring and summer than in autumn and winter. Notably, nodes 2 and 3 exhibited the highest amount of deficiency, which peaked at $-185,100$ kW during the summer, while during the spring, it was observed to be $-178,800$ kW. As shown in Figures 6 and 7, during both the first and second years, the implementation of geothermal technology is restricted solely to nodes 1, 4, and 5, and PV technology is exclusively installed at nodes 2, 3, and 6. With respect to the quantity of electricity generated, geothermal technology produces 271,164 kW during the summer seasons in nodes 1 and 5, and PV technology generates 422,100 kW of electricity during the spring and summer seasons.

Figure 5 depicts the quantity of heat production, demand, and shortage over the four seasons in the first year. The findings demonstrate that various technologies, including geothermal, boiler, CHP, and ST, all generate heat. Notably, geothermal technology produces the highest amount of heat when compared to other technologies. It is worth noting that the contribution of the CHP technology to heat production was observed only during the winter season, and specifically in nodes 2, 3, and 6. Furthermore, Figure 5(d) highlights that the highest heat demand and significant shortage occur during winter. On average, the geothermal technology produced the highest amount of heat, with an average value of 16,771 kW during the winter, followed by the boiler technology, which produced an average of 7,996 kW. In contrast, the ST technology produced an average of 201 kW, while the CHP technology produced an average of 2,386 kW.

Figure S5 in the SI file illustrates the heat production, demand, and shortage during the second year across all four seasons. The figure highlights the installation locations for various technologies, including the boiler, CHP, and solar ST systems

at nodes 2, 3, and 6, respectively. Additionally, geothermal systems are installed at nodes 1, 4, and 5, as indicated in the figure. Figure S5(d) indicates that consistent with the first year, the winter season in the second year has the highest heat demand, with a comparable magnitude to that observed in the previous year. Node 2 has the highest recorded heat demand of 17,165 kW, while the highest heat shortage of 8,945 kW is observed at node 3. Notably, node 4, where the geothermal technology is installed, exhibits the highest heat production of 16,606 kW.

Figure S7 depicts the quantity of cool production, demand, and shortage during the first year. According to Figure S7, the highest cool demand occurs during the summer and spring seasons, with node 1 having the highest demand at 106,076 kW. Also, as shown in Figure S7(b), there is a shortage at nodes 1, 2, and 5 during the summer due to the high demand. All cold production technologies, including ST, EC, and AC, are installed during summer. Comparing the results, the ST technology, which is only installed during summer at node 2, produces the lowest amount of cool at 14 kW, while the EC technology produces the highest amount of cool at node 3 with a magnitude of 107,507 kW.

Figure S6 in the SI file presents valuable insights into the different technologies' cool demand, production, and shortage. The findings reveal that there is no shortage of cool demand during spring, autumn, and winter, and equipment production is sufficient to meet the demand. However, in the summer season, as depicted in Figure S6(b), despite the maximum production of technologies, there is a shortage of cool in nodes 2, 3, and 6. The most significant shortage and highest cool demand during the summer occur at node 2, with a magnitude of $-14,689$ kW, and at node 1, with a magnitude of 107,089 kW, respectively. Notably, EC technology produces more than other technologies, as evident from the results in Figure S6.

Figure S8 shows the solar radiation data for the first and second years. Both years exhibit a peak in solar radiation intensity of 0.85 kWh/m² around noon. Additionally, Figures S8 demonstrate that the highest electricity generation by PV technology occurs between 12 and 5 pm, with a magnitude of 42,000 and 63,000 kW for the first and second years, respectively. These figures only display PV production rates during spring and autumn, as PV production remains constant throughout the seasons of each half of the year with no significant variation in PV production rates between the seasons within each half of the year.

Moreover, Figure S8 suggest that PV production rates are higher during spring and summer compared to autumn and winter. Overall, the results indicate a positive correlation between solar radiation and PV production rates. Thus, higher solar radiation leads to higher electricity generation by PV technology.

4.3. Sensitivity Analysis

A comprehensive sensitivity analysis is crucial for striking the right equilibrium between energy demand and the cost of the MG. This evaluation aids in achieving a cost-effective operation of the MG while fulfilling the energy requirements of its

users. Figure 6 depicts the relationship between changes in energy demand and the objective function and operation cost through a sensitivity analysis. As it is shown, there is a positive correlation between energy demand and the operating cost of the MG and objective function. This correlation can be attributed to various factors, e.g., increase in production cost, storage cost, infrastructure cost, fuel and maintenance costs, labor costs, and energy storage costs. Note that the vertical axes in Figures 6 and 7 represent the values that have been normalized between 0 and 1. Therefore, they are dimensionless.

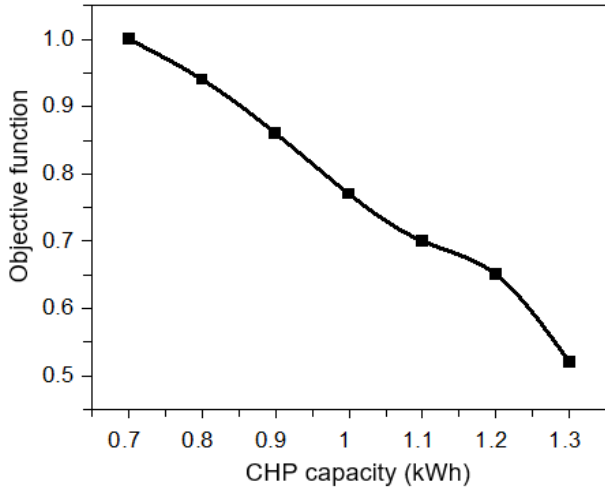


Figure 7. Capacity change v.s. objective function (horizontal axis shows the percentage of CHP capacity changes).

Figure 7 depicts the results of CHP capacity changes versus objective function, showing an inverse relationship between the capacity of CHP and the objective function value, which aimed to minimize the total costs of the MG. Increasing the CHP capacity decreases the objective function value and greenhouse gas emissions since CHP offers enhanced heat and power generation efficiency, leading to reduced fuel consumption and a decreased dependency on conventional power plants and boilers and, ultimately, lower total costs.

5. Conclusions

This study presents a novel approach for optimizing DESs by formulating a MILP model. The model considers a range of renewable energy sources and optimal sizing of technologies and aims to minimize both total costs and GHG emissions while satisfying relevant constraints. Additionally, the model incorporates practical factors such as electricity transmission, heat and cooling generation, natural gas requirements, and limitations to provide a realistic and comprehensive framework.

The proposed model was verified and validated through a real case study, demonstrating its effectiveness in optimizing the performance of DES over a two-year time horizon. The study's results indicate that the optimal amount of buying, selling, producing technology, and transferring electricity between

nodes can be obtained through the model. Notably, the results suggest that the maximum available area was utilized for installing ST technology due to its low cost, leading to installing six CHP units, one Photovoltaic (PV) unit, three boilers, three ST units, six ACs, and six ECs nodes.

This study contributes to developing a comprehensive mathematical model that integrates device capability, optimal total system cost, and optimal operation while considering various renewable energy sources and their energy requirements. Furthermore, incorporating practical factors provides a more realistic and practical model that can contribute to creating efficient and cost-effective DESs.

Future research could enhance the proposed model by integrating customer satisfaction and uncertainty in demand and production scenarios to refine the model further. In addition to integrating customer satisfaction and uncertainty in demand and production scenarios, future research could explore the use of advanced optimization techniques, such as stochastic optimization or dynamic programming to improve the model's performance. Finally, the proposed model can be integrated into a decision support tool that can assist policymakers, planners, and stakeholders in making informed decisions about the design and operation of DESs.

Appendix A. Nomenclature

The proposed model is developed using the nomenclatures outlined below.

Indices

y	Years
t	Periods
h	Hours
l	Types of CHP
b	Types of boilers
$n \& n'$	Nodes

Parameters

C_1^{CHP}	The operational cost of CHP type l in year y , period t , hour h , and node n (\$/kWh)
C_1^{PV}	The operational cost of PV in year y , period t , hour h , and node n (\$/kWh)
C_1^{ST}	The operational cost of ST in year y , period t , hour h , and node n (\$/kWh)
C_1^B	The operational cost of boiler type b in year y , period t , hour h , and node n (\$/kWh)
C_1^{AC}	The operational cost of AC in year y , period t , hour h , and node n (\$/kWh)
C_1^{EC}	The operational cost of EC in year y , period t , hour h , and node n (\$/kWh)
C_l^{CHP}	The capital investment cost for CHP l (\$/kW)
C^{PV}	The capital investment cost for PV (\$/kW)
C^{ST}	The capital investment cost for ST (\$/kW)
C_b^B	The capital investment cost for boiler type b (\$/kW)
C^{AC}	The capital investment cost for AC (\$/kW)
C^{EC}	The capital investment cost for EC (\$/kW)

$C_{n,n'}$	Wiring cost between node n and n' (\$/kW)
$C_{y,t,h,l,n,n'}^{TRCHP}$	Cost of transmission by CHP l from node n to node n' in year y , period t , and hour h (\$)
$C_{y,t,h,l,n,n'}^{TRPV}$	Cost of transmission by PV from node n to node n' in year y , period t , and hour h (\$)
Pen^H	Penalty for unmet heat demand (\$/kWh)
Pen^C	Penalty for cool unmet demand (\$/kWh)
Pen^E	Penalty for unmet electrical demand (\$/kWh)
PEN^{CA}	Amount of emission penalty per gram of carbon (\$/kWh)
θ_l^{CHPE}	CHP electrical production efficiency coefficient type l (%)
β_l^{CHP}	CHP heat production efficiency coefficient type l (%)
WA_n^{AC}	The capacity of AC in node n (kWh)
WA_n^{EC}	The capacity of EC in node n (kWh)
WA_n^B	The capacity of boiler type b in node n (kWh)
WA_l^{CHPE}	Electrical capacity of CHP type l (kWh)
WAH_l^{CHP}	Heat capacity of CHP type l (kWh)
WAH_n^G	Heat capacity of Geothermal in node n (kWh)
WA_n^G	Electrical capacity of Geothermal in node n (kWh)
COP^{AC}	Coefficient of performance for AC
$Dem_{y,t,h,n}^E$	Electric demand in node n , year y , period t , and hour h (kWh)
$DH_{y,t,h,n}$	Heat demand in node n , year y , period t , and hour h (kWh)
$DH_{y,t,h,n}^{AC}$	Heat demand for AC in node n , year y , period t , and hour h (kWh)
$DC_{y,t,h,n}$	Cool demand in node n , year y , period t , and hour h (kWh)
RA_h	PV radiation per hour h (kWh/m ²)
$DI_{n,n'}$	The distance between node n and n' (m)
LB_n^{PV}	The minimum acceptable level for PV installation in node n (m ²)
UP_n^{PV}	The maximum acceptable level for PV installation in node n (m ²)
LB_n^{ST}	The minimum level allowed to install ST in node n (m ²)
UB_n^{ST}	The maximum level allowed to install ST in node n (m ²)
HR_l	Heat to power ratio for CHP type l
$UP_{y,t,h,n}^{DEM}$	Percentage of electricity demand in year y , period t , hour h , and node n (kWh)
$UP_{y,t,h,n}^{PE}$	Percentage of electricity purchased in year y , period t , hour h , and node n (kWh)
$UP_{y,t,h,n}^{DEC}$	Percentage of cool demand in year y , period t , hour h , and node n (%)
$UP_{y,t,h,n}^{DEH}$	Percentage of heat demand in year y , period t , hour h , and node n (%)
γ_n^G	Geothermal installation parameter in node n
α	The conversion factor of CO ₂ production per kWh of heat production by the boiler
δ	The conversion factor of CO ₂ production per kWh of electricity production by CHP
μ	The conversion factor of CO ₂ production per kWh of heat production by CHP
BM	Big number

Continuous Variables

C_{inv}	Total investment costs (\$)
C_{op}	Operating and maintenance costs (\$)
C_{mis}	Total emission cost (\$)
C_{TR}	Total electricity transfer cost (\$)
MS_n^{PV}	The installed surface of PV in node n (m ²)
MS_n^{ST}	The installed surface of ST in node n (m ²)
$AE_{y,t,h,l,n}^{CHP}$	Amount of electricity sold to the grid by CHP l in year y , period t , hour h , and node n (kWh)
$AE_{y,t,h,n}^{PV}$	Amount of electricity sold to the grid by PV in year y , period t , hour h , and node n (kWh)
$UM_{y,t,h,n}^E$	Amount of unmet electricity demand in year y , period t , hour h , and node n (kWh)
$UM_{y,t,h,n}^H$	Amount of unmet heat demand in year y , period t , hour h , and node n (kWh)
$UM_{y,t,h,n}^C$	Amount of cool unmet demand in year y , period t , hour h , and node n (kWh)
$TR_{y,t,h,l,n,n'}^{CHP}$	The power transfer rate by CHP l from node n to node n' in year y , period t , and hour h (kWh)
$TR_{y,t,h,n,n'}^{PV}$	The power transfer rate by PV from node n to node n' in year y , period t , and hour h (kWh)
$PE_{y,t,h,n}$	Purchased electricity from natural grid in year y , period t , hour h , and node n (kWh)
$OP_{y,t,h,l,n}^{CHP}$	The amount of CHP electricity production type l in year y , period t , hour h , and node n (kW)
$OP_{y,t,h,n}^{PV}$	The amount of PV electricity production in year y , period t , hour h , and node n (kW)
$OH_{y,t,h,b,n}^B$	The amount of boiler heat production type b in year y , period t , hour h , and node n (kW)
$OH_{y,t,h,n}^{ST}$	The amount of ST heat production in year y , period t , hour h , and node n (kW)
$OH_{y,t,h,l,n}^{CHP}$	The amount of CHP heat production type l in year y , period t , hour h , and node n (kW)
$OH_{y,t,h,n}^G$	The amount of geothermal heat production in year y , period t , hour h , and node n (kW)
$OP_{y,t,h,n}^G$	The amount of geothermal electricity production in year y , period t , hour h , and node n (kW)
$OC_{y,t,h,n}^{AC}$	The amount of AC production in year y , period t , hour h , and node n (kW)
$OC_{y,t,h,n}^{EC}$	The amount of EC production in year y , period t , hour h , and node n (kW)
$OC_{y,t,h,n}^{ST}$	The amount of ST cool production in year y , period t , hour h , and node n (kW)

Binary Variables

$X_{l,n}^{CHP}$	The binary variable that decides whether to install CHP type l on node n
W_n^{PV}	The binary variable that decides whether to install PV on node n
λ_n^{ST}	The binary variable that decides whether to install ST on node n
$Y_{b,n}^B$	The binary variable that decides whether to install boiler type b on node n
\mathcal{Q}_n^{AC}	The binary variable that decides whether to

install AC on node n

g_n^{EC} The binary variable that decides whether to install EC on node n

$U_{n,n'}$ The binary variable decides whether to install a wire between n and n'

References

- Adewole, A.C., Rajapakse, A.D., Ouellette, D. and Forsyth, P. (2022). Protection of active distribution networks incorporating microgrids with multi-technology distributed energy resources. *Electr. Power Syst. Res.*, 202, 107575. <https://doi.org/10.1016/j.epsr.2021.107575>
- Águila, A., Ortiz, L., Orizondo, R. and López, G. (2021). Optimal location and dimensioning of capacitors in microgrids using a multicriteria decision algorithm. *Heliyon*, 7(9), e08061. <https://doi.org/10.1016/j.heliyon.2021.e08061>
- Ahmadi, S.E. and Rezaei, N. (2021). An IGDT-based robust optimization model for optimal operational planning of cooperative microgrid clusters: A normal boundary intersection multi-objective approach. *Int. J. Electr. Power & Energy Syst.*, 127, 106634. <https://doi.org/10.1016/j.ijepes.2020.106634>
- Ahmethodzic, L. and Music, M. (2021). Comprehensive review of trends in microgrid control. *Renew. Energy Focus*, 38, 84-96. <https://doi.org/10.1016/j.ref.2021.07.003>
- Aluisio, B., Dicorato, M., Ferrini, I., Forte, G., Sbrizzai, R. and Trovato, M. (2021). Planning and reliability of DC microgrid configurations for Electric Vehicle Supply Infrastructure. *Int. J. Electr. Power & Energy Syst.*, 131, 107104. <https://doi.org/10.1016/j.ijepes.2021.107104>
- Amanatidou, E., Samiotis, G., Trikoilidou, E., Tsikritzis, L. and Taouanidis, N. (2023). Centennial assessment of greenhouse gases emissions of young and old hydroelectric reservoir in Mediterranean mainland. *J. Environ. Inf.*, 41(1), 27-36 <https://doi.org/10.3808/jei.202300485>
- Anyaocha, K.E. and Zhang, D.L. (2022). Transition from fossil-fuel to renewable-energy-based smallholder bioeconomy: Techno-economic analyses of two oil palm production systems. *Chem. Eng. J. Adv.*, 10, 100270. <https://doi.org/10.1016/j.cej.2022.100270>
- Balasubramanian, R., Abishek, A., Gobinath, S. and Jaivignesh, K. (2022). Alternative fuel: Hydrogen and its thermodynamic behaviour. *J. Hum. Earth, Future*, 3(2), 195-203. <https://doi.org/10.28991/HEF-2022-03-02-05>
- Bartels, E.A., Pippia, T. and De Schutter, B. (2022). Influence of hydrogen on grid investments for smart microgrids. *Int. J. Electr. Power & Energy Syst.*, 141, 107968. <https://doi.org/10.1016/j.ijepes.2022.107968>
- Basu, M. (2021). Heat and power generation augmentation planning of isolated microgrid. *Energy*, 223, 120062. <https://doi.org/10.1016/j.energy.2021.120062>
- Bayati, N., Balouji, E., Baghaee, H.R., Hajizadeh, A., Soltani, M., Lin, Z. and Savaghebi, M. (2022). Locating high-impedance faults in DC microgrid clusters using support vector machines. *Appl. Energy*, 308, 118338. <https://doi.org/10.1016/j.apenergy.2021.118338>
- Bukar, A.L., Tan, C.W., Yiew, L.K., Ayop, R. and Tan, W.S. (2020). A rule-based energy management scheme for long-term optimal capacity planning of grid-independent microgrid optimized by multi-objective grasshopper optimization algorithm. *Energy Convers. Manage.*, 221, 113161. <https://doi.org/10.1016/j.enconman.2020.113161>
- Bukar, A.L., Tan, C.W., Said, D.M., Dobi, A.M., Ayop, R. and Alsharif, A. (2022). Energy management strategy and capacity planning of an autonomous microgrid: Performance comparison of metaheuristic optimization searching techniques. *Renew. Energy Focus*, 40, 48-66. <https://doi.org/10.1016/j.ref.2021.11.004>
- Califano, M., Sorrentino, M., Rosen, M.A. and Pianese, C. (2022). Optimal heat and power management of a reversible solid oxide cell based microgrid for effective technoeconomic hydrogen consumption and storage. *Appl. Energy*, 319, 119268. <https://doi.org/10.1016/j.apenergy.2022.119268>
- Chaudhary, G., Lamb, J.J., Burheim, O.S. and Austbø, B. (2021). Review of energy storage and energy management system control strategies in microgrids. *Energy*, 14(16), 4929. <https://doi.org/10.3390/en14164929>
- Chen, X., Zhou, J.Y., Shi, M.X., Chen, Y. and Wen, J.Y. (2022). Distributed resilient control against denial of service attacks in DC microgrids with constant power load. *Renew. Sust. Energy Rev.*, 153, 111792. <https://doi.org/10.1016/j.rser.2021.111792>
- Demirhan, H. (2022). Solar photovoltaic utilization in electricity generation to tackle climate change. *J. Environ. Inf.*, 40(1), 41-55. <https://doi.org/10.3808/jei.202200475>
- Dougier, N., Garambois, P., Gomand, J. and Roucoules, L. (2021). Multi-objective non-weighted optimization to explore new efficient design of electrical microgrids. *Appl. Energy*, 304, 117758. <https://doi.org/10.1016/j.apenergy.2021.117758>
- Dumas, J., Dakir, S., Liu, C. and Cornélusse, B. (2021). Coordination of operational planning and real-time optimization in microgrids. *Electr. Power Syst. Res.*, 190, 106634. <https://doi.org/10.1016/j.epsr.2020.106634>
- Fioriti, D., Poli, D., Duenas-Martinez, P. and Perez-Arriaga, I. (2021). Multi-year stochastic planning of off-grid microgrids subject to significant load growth uncertainty: overcoming single-year methodologies. *Electr. Power Syst. Res.*, 194, 107053. <https://doi.org/10.1016/j.epsr.2021.107053>
- Gabriel, L.F.G., Ruiz-Cruz, R., Coss y Leon Monterde, H.J., Zúñiga-Grajeda, V., Gurubel-Tun, K.J. and Coronado-Mendoza, A. (2022). Optimizing the penetration of standalone microgrid, incorporating demand side management as a guiding principle. *Energy Rep.*, 8, 2712-2725. <https://doi.org/10.1016/j.egy.2022.01.192>
- Giacosa, G. and Walker, T.R. (2022). A policy perspective on Nova Scotia's plans to reduce dependency on fossil fuels for electricity generation and improve air quality. *Cleaner Prod. Lett.*, 3, 100017. <https://doi.org/10.1016/j.clpl.2022.100017>
- Guidentif, T.M.M. and Vuille, F. (2022). Prospects and barriers for microgrids in Switzerland. *Energy Strategy Rev.*, 39, 100776. <https://doi.org/10.1016/j.esr.2021.100776>
- Guo, L., Hou, R.S., Liu, Y.X., Wang, C.S. and Lu, H. (2020). A novel typical day selection method for the robust planning of stand-alone wind-photovoltaic-diesel-battery microgrid. *Appl. Energy*, 263, 114606. <https://doi.org/10.1016/j.apenergy.2020.114606>
- Harrold, D.J.B., Cao, J. and Fan, Z. (2022). Renewable energy integration and microgrid energy trading using multi-agent deep reinforcement learning. *Appl. Energy*, 318, 119151. <https://doi.org/10.1016/j.apenergy.2022.119151>
- Hu, J., Shan, Y., Cheng, K.W. and Islam, S. (2022). Overview of power converter control in microgrids—challenges, advances, and future trends. *IEEE T. Power Electr.*, 37(8), 9907-9922. <https://doi.org/10.1109/TPEL.2022.3159828>
- Jiao, P.H., Chen, J.J., Peng, K., Zhao, Y.L. and Xin, K.F. (2020). Multi-objective mean-semi-entropy model for optimal standalone micro-grid planning with uncertain renewable energy resources. *Energy*, 191, 116497. <https://doi.org/10.1016/j.energy.2019.116497>
- Kiptoo, M.K., Lotfy, M.E., Adewuyi, O.B., Conteh, A., Howlader, A. M. and Senjyu, T. (2020). Integrated approach for optimal technoeconomic planning for high renewable energy-based isolated microgrid considering cost of energy storage and demand response strategies. *Energy Convers. Manage.*, 215, 112917. <https://doi.org/10.1016/j.enconman.2020.112917>
- Kizito, R., Liu, Z.Y., Li, X.P. and Sun, K. (2022). Multi-stage stochastic optimization of islanded utility-microgrids design after natural disasters. *Oper. Res. Perspect.*, 9, 100235. <https://doi.org/10.1016/j.orp.2022.100235>

- Mathiesen, P., Stadler, M., Kleissl, J. and Pecenek, Z. (2021). Techno-economic optimization of islanded microgrids considering intra-hour variability. *Appl. Energy*, 304, 117777. <https://doi.org/10.1016/j.apenergy.2021.117777>
- Mei, H., Li, Y.P., Lv, J., Chen, X.J., Lu, C., Suo, C. and Ma Y. (2022). Development of an integrated method (MGCMs-SCA-FER) for assessing the impacts of climate change: A case study of Jing-Jin-Ji region. *J. Environ. Inf.*, 38(2), 145-161. <https://doi.org/10.3808/jei.202100458>
- O'Neill, D., Yildiz, B. and Bilbao, J. I. (2022). An assessment of electric vehicles and vehicle to grid operations for residential microgrids. *Energy Rep.*, 8, 4104-4116. <https://doi.org/10.1016/j.egy.2022.02.302>
- Oviedo-Cepeda, J.C., Serna-Suárez, I., Osma-Pinto, G., Duarte, C., Solano, J. and Gabbar, H.A. (2020). Design of tariff schemes as demand response mechanisms for stand-alone microgrids planning. *Energy*, 211, 119028. <https://doi.org/10.1016/j.energy.2020.119028>
- Papież, M., Śmiech, S., Frodyma, K. and Borowiec, J. (2022). Decoupling is not enough - Evidence from fossil fuel use in over 130 countries. *J. Cleaner Prod.*, 379(2), 134856. <https://doi.org/10.1016/j.jclepro.2022.134856>
- Phommixay, S., Doumbia, M. L. and Cui, Q. (2021). A two-stage two-layer optimization approach for economic operation of a microgrid under a planned outage. *Sustain. Cities Soc.*, 66, 102675. <https://doi.org/10.1016/j.scs.2020.102675>
- Pinto, R. S., Unsihuay-Vila, C. and Tabarro, F. H. (2021). Coordinated operation and expansion planning for multiple microgrids and active distribution networks under uncertainties. *Appl. Energy*, 297, 117108. <https://doi.org/10.1016/j.apenergy.2021.117108>
- Rios, M. A. and Garces, A. (2022). An optimization model based on the frequency dependent power flow for the secondary control in islanded microgrids. *Comput. Electr. Eng.*, 97, 107617. <https://doi.org/10.1016/j.compeleceng.2021.107617>
- Roy, A., Olivier, J.C., Auger, F., Auvity, B., Schaeffer, E., Bourguet, S., Schiebel, J. and Perret, J. (2021). A combined optimization of the sizing and the energy management of an industrial multi-energy microgrid: Application to a harbour area. *Energy Convers. Manage.: X*, 12, 100107. <https://doi.org/10.1016/j.ecmx.2021.100107>
- Shezan, S.A., Ishraque, M.F., Muyeen, S.M., Arifuzzaman, S.M., Paul, L.C., Das, S.K. and Sarker, S.K. (2022). Effective dispatch strategies assortment according to the effect of the operation for an islanded hybrid microgrid. *Energy Convers. Manage.: X*, 14, 100192. <https://doi.org/10.1016/j.ecmx.2022.100192>
- Tahiri, F. E., Chikh, K. and Khafallah, M. (2021). Optimal management energy system and control strategies for isolated hybrid solar-wind-battery-diesel power system. *Emerging Sci. J.*, 5(2), 111-124. <https://doi.org/10.28991/esj-2021-01262>
- Taraghi Nazloo, H., Babazadeh, R. and Ghanizadeh Bolandi, T. (2023). Developing a mathematical programming model for planning and sizing of grid-connected microgrids. *Renew. Energy Focus*, 44, 212-222. <https://doi.org/10.1016/j.ref.2023.01.001>
- Villa, C. and Henao, F. (2022). Oversizing grid-connected microgrids as a business model—An optimisation assessment approach. *Energy Rep.*, 8, 2100-2118. <https://doi.org/10.1016/j.egy.2022.01.117>
- Wei, J.D., Zhang, Y., Wang, J.X., Cao, X.Y. and Khan, M.A. (2020). Multi-period planning of multi-energy microgrid with multi-type uncertainties using chance constrained information gap decision method. *Appl. Energy*, 260, 114188. <https://doi.org/10.1016/j.apenergy.2019.114188>